Mouse Chromosome Translocations: Visualization and Analysis by Electron Microscopy of the Synaptonemal Complex

Abstract. *Pachytene chromosomes of mice heterozygous for known translocations are clearly depicted by configurations of the synaptonemal complexes in spread (whole mount) preparations. In one autosomal and two* X*-autosome translocations analyzed, breakpoints are identifiable; localization by measurement agrees with mitotic data and shows the translocations to be reciprocal. Synapsis with the* Y *is inhibited in one translocation in which the breakpoint is in the pairing region of the* X.

Electron microscopic studies of pachytene nuclei, in which three-dimensional reconstructions from serial sections (*1–3*), or selectively stained whole mounts spread by surface tension on an aqueous interphase (*4–6*) were used, have shown that the synaptonemal complex (SC) closely parallels bivalent behavior. The lateral elements of the SC are equivalent to the axes of the paired homologs and, thus, may be taken as their analogs (*2*, *3*). This has been shown to be true during synapsis and desynapsis, and for normal chromosomes as well as chromosomal rearrangements (*7*). In particular, three-dimensional reconstructions by Solari of Searle's X-autosome translocation in the mouse (*8*), and by Gillies of inversion 3b in maize (*2*), show that the axial elements follow exactly the pairing configurations expected of the homologous chromosome portions themselves. These observations suggested that it might be feasible to detect and analyze rearrangements at pachytene by studying SC and axial element behavior by means of the electron microscope and a simplified whole mount preparative procedure. To explore such an approach we have taken advantage of the special pattern in pairing behavior of chromosomes known to be heterozygous for rearrangements, and have utilized the superior resolution of the electron microscope for a comparison with analyses made with light microscopic methods.

A spreading technique of Counce and Meyer (*5*) applied to mammalian meiocytes (*6*, *9*) yields full complements of selectively stained SC's in which kinetochores are represented by dense differentiations of the lateral elements of the SC (Fig. 1a). A suspension of testicular cells is spread on the surface of 0.5 percent NaCl; a coated specimen grid is touched to the surface and the adhering cells are fixed with formalin, stained with ethanolic phosphotungstic acid, and observed in the electron microscope [see (*9*) for details]. The application of this simple and rapid method for quantitative karyotyping has shown close correspondence with standard mitotic karyotypes (*6*, *9*). The results are reproducible and demonstrate both biological and mechanical stability of the SC's as evidenced by the constancy of their relative lengths and arm ratios among nuclei and individual animals (*10*). Such evidence validates the method for SC karyotyping and justifies its extension to the analysis of rearrangements.

Using the above method, we have examined preparations from three translocations in the mouse, all of which had earlier been studied genetically and cytologically (*11–16*). Two of these involve the X and chromosome 7, but with breakpoints in markedly different positions in the two rearrangements (R6 and R2); and one is an autosomal translocation (R12). Spread preparations of pachytene spermatocytes from one heterozygous male of each translocation stock were made and quantitated as described elsewhere (*6*, *10*). Experiments were performed as blind tests; the chromosome constitutions of the mouse stocks provided by one of us (L.B.R.) were unknown to the other (M.J.M.) until after the analysis.

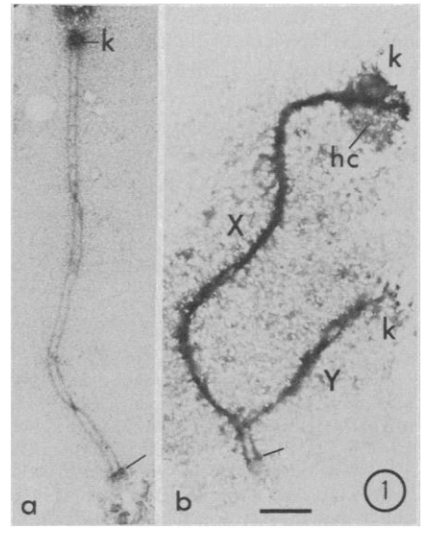

Fig. 1. Electron micrograph of an autosomal SC (a) and XY pair (b) in a spread preparation of mouse pachytene spermatocytes. (a) The SC of each bivalent consists of parallel paired lateral elements which are equivalent to the laterally displaced axes of the synapsed homologous chromosomes, and a thin central element which is often not visible in these preparations. A densely stained differentiation of the SC close to one terminal attachment to the nuclear envelope represents the kinetochore (*k*), and is distinguishable from the attachment plaque (−) at the opposite end. (b) The axial elements of the X and Y chromosomes are thickened, densely staining, and occasionally multiple stranded where they are unpaired. At one end, the axes pair to form the thin lateral elements of a short length of SC which ends on the nuclear envelope in an attachment plaque (−). At an earlier stage, X-Y pairing is more complete, with the SC occupying most of the length of the Y axis. Kinetochores are nearly terminal in the X and Y; paracentromeric heterochromatin (*hc*) often distinguishes that of the X. Scale bar, 1 μm.

The translocations as represented by configurations of the SC's were easily identified with the electron microscope in all preparations and are diagrammatic in their clarity (Figs. 2a, 3a, and 4a, and 2b, 3b, and 4b). In normal preparations (Fig. 1, a and b), as well as in the rearrangements, the X and Y chromosome axes are easily distinguished from autosomal SC's; they are largely unpaired and show distinctive thickenings. However, the autosomes involved in the rearrangements, while known from earlier genetic and mitotic analyses, cannot be identified reliably in the individual examples reported here. In the X-autosome translocations, the breakpoints at which the X and autosome are joined are sharply defined (Figs. 2a and 3a, arrowheads) because of thickening of the X portions. Also, the kinetochore, which is virtually terminal in the mouse (Fig. 1, a and b; *k*), unequivocally identifies proximal and distal segments of the translocation (Figs. 2a and 3a; *k*). In all three instances, the morphological configurations fit exactly those predicted from prior cytogenetic information.

Quantitative estimations were made for comparison with established light microscopic and genetic evidence. Measured breakpoints are presented in Table 1, column 4. For example, in R6, shown in Fig. 2, a and b, 71 percent of the X axis and 22 percent of the No. 7 axis are proximal to the respective breakpoints. These figures compare with 81 and 27 percent, respectively, independently estimated from banded mitotic chromosomes (Table 1, column 5); the data for the other translocations show even better agreement. Observed differences, though small, may be partly attributable to uncertainties in locating breakpoints in the mitotic metaphase preparations, especially where these are not in or near a well-defined narrow band.

Axial lengths (that is, lateral elements of the SC) of the chromosomes involved in each example of the three translocations were measured. For purposes of comparison with nontranslocated

homologs, the chromosomes involved in the translocations were "reconstructed" by adding the lengths of the two separated segments of their lateral elements. This could be done most accurately for the X-autosome translocations where the breakpoints are clearly identifiable (Figs. 2a and 3a; arrowheads).

"Reconstructed" chromosomes may be compared with their intact homologs (Table 1). In the case of the X, which has no homolog in male cells, a reasonable comparison may be made between relative length of the reconstructed X and relative length of the X in normal nuclei. However, such a comparison may not be entirely reliable because the relative length of the normal X may vary during pachytene (*17*). Nevertheless, reconstructed translocation X chromosome and autosome axes in general show satis-

Table 1. Quantitative comparisons of breakpoints and measured lengths of three chromosome translocations in the mouse. EM, electron microscopy; LM, light microscopy.

Translocation stock	Abbreviation	Translocated chromosome No.	Breakpoint*		Measured length (μm)	
			EM	LM†	Reconstructed chromosome axis‡	Nontranslocated chromosome axis§
T(X;7)6Rℓ	R6	X	0.71	0.81	[6.2]‖	[6.5]¶
T(X;7)6Rℓ	R6	7	0.22	0.27	7.3	7.8
T(X;7)2Rℓ	R2	X	0.28	0.22#	[5.7]‖	[6.5]¶
T(X;7)2Rℓ	R2	7	0.60	0.66#	9.9	9.4
T(10;18)12Rℓ	R12	10	0.79	0.78	8.0	8.6
T(10;18)12Rℓ	R12	18	0.49	0.50	5.7	5.8

*The breakpoint is designated as the fraction of the "reconstructed" chromosome (axis) length represented by the kinetochore-bearing (proximal) arm of the translocation (mean values are shown for LM). †Data are from banded mitotic karyotypes, prepared from kidney cultures of adult mice. For each of the two T(X;A)'s, measurements were made in six cells: three banded with quinacrine mustard, and three with Giemsa. For R12, chromosomes were measured in three cells, all quinacrine mustard banded. Somatic and SC measurements were made independently by different observers and were not compared until analyses were complete. ‡The chromosomes involved in the translocation were "reconstructed" by adding axis lengths of the two separated segments. §The nontranslocated chromosome axis is the continuous lateral element that is partner in the SC to its homologous proximal and distal translocated segments. ‖Length is expressed as the percentage relative length, that is, the length of X dividied by [Σ autosomal SC length + ½ (X axis + Y axis)]. ¶Mean of X axis relative lengths from seven pachytene spermatocyte karyotypes of a normal mouse stock. #These measurements assume breakpoint locations in XA2 and 7D3. A slightly different combination of breakpoints is also possible (*11*).

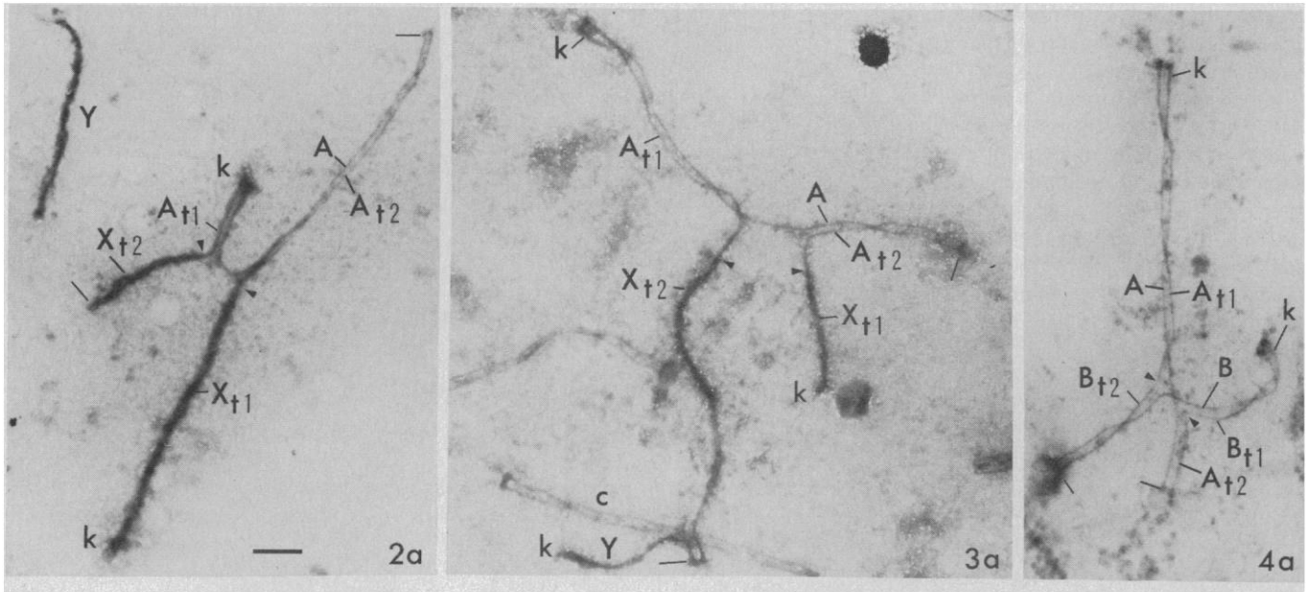

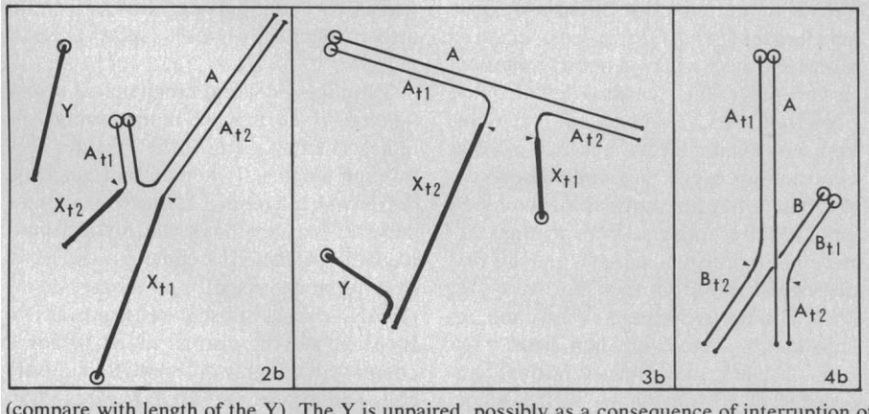

Figs. 2a, 3a, and 4a. Electron micrographs of spread pachytene translocation pairing figures from three different translocations in the mouse. Symbols: A, nontranslocated autosomal lateral element (axis); A_{t1} and A_{t2}, axes of translocated portions of autosome; B, nontranslocated axis of second autosome; B_{t1} and B_{t2}, axes of translocated portions of second autosome; X_{t1} and X_{t2}, translocated portions of X axis; c, indifferent autosomal SC; k, kinetochore; Y, Y axis; (−), distal attachment plaque; arrowheads, translocation breakpoints. Scale bar, 1 μm. Fig. 2. (a) T(X;7)6Rℓ (or R6). Translocation trivalent: see schematic diagram (Fig. 2b). In the smaller translocation product, A_{t1} X_{t2}, the distal (X_{t2}) segment is shorter than the full pairing region (compare with length of the Y). The Y is unpaired, possibly as a consequence of interruption of the X pairing region. Fig. 3. (a) T(X;7)2Rℓ (or R2). Translocation quadrivalent: see schematic diagram (Fig. 3b). In the long translocation product $A_{t1}X_{t2}$, and X_{t2} portion consists of the distal 3/4 of the X. The X and Y are terminally paired by a short remaining segment of SC. An autosomal SC accidentally crosses the XY pair. Autosomal portions of the two translocated axes have either failed to pair with, or have stripped away from the nontranslocated No. 7 axis for a short distance near the translocation breakpoints (arrowheads). Fig. 4. (a) T(10;18)12Rℓ (or R12). Translocation quadrivalent: see schematic diagram (Fig. 4b). Because the lateral elements (axes) of the two autosomes are indistinguishable, the breakpoints can only be approximated. However, the estimates agree well with data from mitotic chromosomes (Table 1). The dense granule in the proximal third of one SC is identified as a recombination nodule (*22*); other SC's in this nucleus also contain them. Figs. 2b, 3b, and 4b. Schematic diagrams, drawn to scale, of the translocation figures shown in Figs. 2a, 3a, and 4a, respectively.

factory correspondence with their intact counterparts.

The breakpoints in the autosomal translocation R12 (Fig. 4a) are less certain because there are no morphological differences in the translocated axes as there are in the X-autosome translocations. However, the sharp bend that was taken as the putative breakpoint is evidently correct, as judged both by the close agreement with somatic breakpoint measurements and the correspondence of the reconstructed axes with the nontranslocated axes (Table 1). Moreover, the sum of the translocation axes ($A_{t1} + A_{t2} + B_{t1} + B_{t2} = 13.7$ μm) compares well with the sum of the nontranslocation axes ($A + B = 14.4$ μm). Since small differences could be due to stretching, the data in general indicate that none of the three translocations involves major chromosome losses or gains, supporting the earlier suggestions (*12, 16*) that they are reciprocal. A more precise statement requires further analyses of larger samples.

Autosomal SC formation, an index of synapsis, is apparently not altered significantly in the three translocations. (The separation of autosomal regions near the breakpoint in Fig. 3a may be a technical artifact.) On the other hand, in all cells so far examined, pairing of the X and Y is blocked in R6 (Fig. 2a), but not in R2 (Fig. 3a). Normally, the X and Y are paired distally to form a length of SC (*18*). At early pachytene, the distal third of the X axis and most of the Y are involved; as pachytene progresses, the synapsed region is greatly reduced (Fig. 1b). In R6, the break occurs in the distal third of the X, that is, in the pairing region. In R2, the break is in the proximal portion and evidently does not affect the pairing region. Conceivably, translocations involving a breakpoint within the pairing region of the X could inhibit synapsis with the Y. This is consistent with observations on Ohno and Cattanach's translocation in the mouse (*19*), where occasional Y univalents indicate irregular XY pairing. The breakpoint is genetically close to that of R6 and therefore presumably falls within what has been identified here as the pairing portion of the X. On the other hand, in Searle's translocation (*20*), where the breakpoint is just proximal to the pairing region of the X, the X and Y are observed to pair (*8*). All T(X;A)'s are male sterile, with spermatogenesis ceasing after pachytene (*14, 21*).

Our results verify the nature of the three translocations by a relatively simple procedure that graphically demonstrates the rearrangements at pachytene, permits mapping of the breakpoints, yields additional confirmation of reciprocity, and provides information about meiotic consequences of the rearrangement, such as pairing abnormalities of the X and Y. The method promises to be valuable also in analyzing other chromosomal rearrangements, such as deletions and inversions.

MONTROSE J. MOSES

Department of Anatomy, Duke University Medical Center, Durham, North Carolina 27710

LIANE B. RUSSELL
N. L. A. CACHEIRO

Biology Division, Oak Ridge National Laboratory, Oak Ridge, Tennessee 37830

References and Notes

1. R. Wettstein and J. R. Sotelo, *J. Microsc. (Paris)* **6**, 557 (1967); P. B. Moens, *Chromosoma* **28**, 1 (1969); C. B. Gillies, *ibid.* **36**, 119 (1972); P. B. Moens and F. O. Perkins, *Science* **166**, 1289 (1969); A. T. C. Carpenter, *Chromosoma* **51**, 157 (1975); S. Rasmussen, *ibid.* **54**, 245 (1976).
2. C. B. Gillies, *Chromosoma* **43**, 145 (1973).
3. P. B. Moens, *Cold Spring Harbor Symp. Quant. Biol.* **38**, 99 (1974).
4. D. E. Comings and T. A. Okada, *Chromosoma* **30**, 269 (1970); A. J. Solari, *ibid.* **39**, 237 (1972).
5. S. J. Counce and G. F. Meyer, *ibid.* **44**, 231 (1973).
6. M. J. Moses and S. J. Counce, in *Symposium on Mechanisms in Recombination*, R. Grell, Ed. (Plenum, New York, 1974), pp. 385–390; ———, D. F. Paulson, *Science* **187**, 363 (1975).
7. Some of the results reported here were presented at the 1975 meeting of the Genetics Society of America [see M. J. Moses, S. J. Counce, A. E. Hamilton, P. A. Karatsis, L. B. Russell, *Genetics* **80**, s58 (1975)].
8. A. J. Solari, *Chromosoma* **34**, 99 (1971).
9. M. J. Moses, *ibid.* **60**, 99 (1977).
10. ———, T. Gambling, G. Slatton, F. Starmer, *ibid.* p. 345.
11. Genetic analysis indicates that in T(X;7)6Rℓ, abbreviated as R6, the autosomal breakpoint is about 2 centimorgans proximal to the *p* locus (*12*), and the X-chromosome breakpoint about 7 centimorgans distal to the *Ta* locus (*13, 14*). Cytologically, by means of banding techniques, the breakpoints have been located in 7B3 and XF1, respectively (*15*). In T(X;7)2Rℓ, or R2, no recombination has to date been observed between the autosomal breakpoint and the *c* locus (*12*); the X-chromosome breakpoint lies between *Ta* and *spf* but closer to the latter (*13, 14*). The cytological breakpoints are at 7D3 and XA2 (or, at 7E1 and XA3), respectively (*14*). The autosomal translocation, T(10;18)12Rℓ, or R12, has its chromosome-10 breakpoint at or very near the Sℓ locus in 10D, with the other breakpoint cytologically located in 18D (*16*).
12. L. B. Russell and C. S. Montgomery, *Genetics* **64**, 281 (1970).
13. ———, *ibid.* **54**, 358 (1966).
14. L. B. Russell, unpublished data.
15. ——— and N. L. A. Cacheiro, *Oak Ridge National Laboratory, Biological Division of Annual Projects Report* (ORNL-4993, Oak Ridge, Tenn., June 1974), p. 125.
16. N. C. A. Cacheiro and L. B. Russell, *Genet. Res.* **25**, 193 (1975).
17. M. J. Moses, *Chromosoma* **60**, 127 (1977).
18. A. J. Solari, *ibid.* **29**, 217 (1970); M. J. Moses, unpublished data.
19. S. Ohno and B. M. Cattanach, *Cytogenetics* **1**, 129 (1962).
20. A. G. Searle, *Heredity* **17**, 297 (1962); C. E. Ford and E. P. Evans, *Cytogenetics* **3**, 295 (1964).
21. L. B. Russell and C. S. Montgomery, *Genetics* **63**, 103 (1969).
22. A. T. C. Carpenter, *Proc. Natl. Acad. Sci. U.S.A.* **72**, 3186 (1975).
23. We thank T. Gambling and G. Slatton for technical assistance, and S. J. Counce and A. J. Solari for numerous helpful discussions. This research was in part supported by NSF grant GB-40562, and NIH grants 5-S01-RR-05404 and CA-14236 to Duke University, and in part sponsored by ERDA under contract with Union Carbide Corp.

29 October 1976; revised 7 December 1976

Evidence for Abnormal Heart Induction in Cardiac-Mutant Salamanders (*Ambystoma mexicanum*)

Abstract. *Homozygosity for simple recessive gene* c *in axolotl embryos results in the absence of a heartbeat. Gene* c *alters the morphology of the mutant anterior endoderm—the primary heart inductor.*

In an imported stock of dark Mexican salamanders, *Ambystoma mexicanum*, a naturally occurring genetic mutation, designated *c* for "cardiac lethal," has been reported. Homozygous recessive embryos exhibit a total absence of heart contractions even though initial heart development appears normal. Mutant (*c*/*c*) embryos are obtained from matings between heterozygous parents and are first distinguishable from their normal (+/+; +/*c*) siblings at Schreckenberg and Jacobson (*3*) stage 34, when heart contractions first develop in normal embryos. The mutant hearts at this stage, upon gross examination, appear structurally normal but fail to beat. Subsequently, the heart becomes distended and remains thin-walled, and the embryo acquires ascites. Mutants survive for about 20 days beyond the time when the heart would normally have begun to beat; they exhibit normal swimming movements, which indicates that gene *c* does not affect skeletal muscle.

Morphological and biochemical investigations of normal and mutant embryonic hearts from stage 34 (heartbeat stage) through stage 41 (when mutant embryos die) have been reported. Electron microscopy reveals that the normal myocardium has well-organized sarcomeres at stage 34 (the heartbeat stage), and numerous intercalated discs subsequently appear (*4*). By stage 41, the normal myocardium is composed of highly differentiated muscle cells and shows extensive trabeculation (*5*). The mutant myocardium throughout development remains only one-cell-layer thick with no indication of developing trabeculae. Mutant cells at stage 34 have a few sparcely scattered thick (150 Å) and thin (60 Å) filaments along with what appear to be Z bodies. A partial organiza-